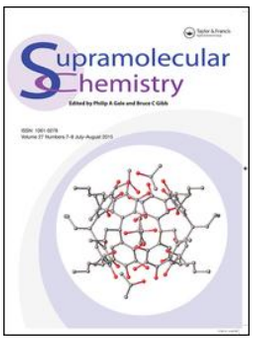

Supramolecular Chemistry

ISSN: 1061-0278 (Print) 1029-0478 (Online) Journal homepage: http://www.tandfonline.com/loi/gsch20

Targeted structural modification of spin crossover complexes: pyridine vs pyrazine

Humphrey L. C. Feltham, Matthew G. Cowan, Jonathan A. Kitchen, Guy N. L. Jameson & Sally Brooker

To cite this article: Humphrey L. C. Feltham, Matthew G. Cowan, Jonathan A. Kitchen, Guy N. L. Jameson & Sally Brooker (2017): Targeted structural modification of spin crossover complexes: pyridine vs pyrazine, Supramolecular Chemistry, DOI: 10.1080/10610278.2017.1358449

To link to this article: http://dx.doi.org/10.1080/10610278.2017.1358449

SUPRAMOLECULAR CHEMISTRY, 2017
https://doi.org/10.1080/10610278.2017.1358449

Taylor & Francis
Taylor & Francis Group

Targeted structural modification of spin crossover complexes: pyridine vs pyrazine

Humphrey L. C. Feltham, Matthew G. Cowan[†], Jonathan A. Kitchen[‡], Guy N. L. Jameson[¶] and Sally Brooker*

Department of Chemistry, MacDiarmid Institute for Advanced Materials and Nanotechnology, University of Otago, Dunedin, New Zealand

ABSTRACT

2-(Aminomethyl)pyrazine has been prepared in five steps from 2-pyrazine carboxylic acid. From this key amine, two new bis-terdentate triazole-based ligands which feature pendant *pyrazine* groups, **P_ZMAT** and **P_ZMPT** (4-amino- and 4-pyrrolyl-3,5-bis{[(2-pyrazylmethyl)amino]methyl}-4H-1,2,4-triazole, respectively), and two dinuclear complexes of them, $[Fe^{II}_2(\mathbf{P_ZMAT})_2](BF_4)_4{\cdot}MeOH{\cdot}2H_2O$ (**1**·MeOH·$2H_2O$) and $[Fe^{II}_2(\mathbf{P_ZMPT})_2](BF_4)_4{\cdot}3H_2O$ (**2**·$3H_2O$), have been prepared. A structure determination at 100 K on **2**·3.5MeCN confirmed that the ligands adopt the expected binding mode, providing all twelve donors to the two iron(II) centres and two N^1,N^2-triazole bridges between them. Both undergo gradual incomplete spin transitions: at room temperature **1**·MeOH·$2H_2O$ and **2**·$3H_2O$ are approximately two-thirds to three-quarters [HS-HS], dropping to mostly '[HS-LS]' at 50 K. The structure determination and Mössbauer spectroscopy of **2** qualitatively support this. These findings are consistent with the pendant pyrazines providing a somewhat higher field strength than the pendant pyridines do in the analogous **PMRT** complexes.

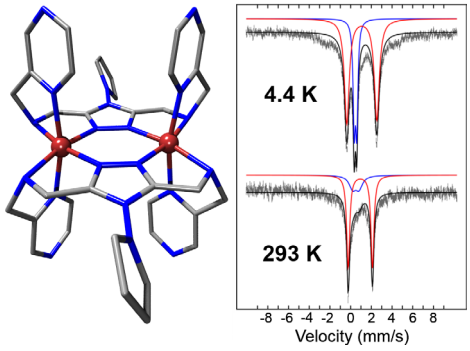

ARTICLE HISTORY
Received 28 May 2017
Accepted 18 July 2017

KEYWORDS
Spin crossover; pyrazine; triazole; iron(II); dinuclear; 2-(aminomethyl)pyrazine; heterocycle

Introduction

Spin crossover (SCO) is a phenomenon observed in some complexes of d^4 to d^7 transition metal ions whereby an external perturbation can switch the metal ion between the high-spin (HS) or low-spin (LS) states (*1*). The transition is usually accompanied by changes in the structural, optical, vibrational and magnetic properties of the complex. This has made SCO-active materials interesting candidates for use in displays and sensors, as well as in applications requiring binary 'on/off'-type functionality, such as molecular data storage (*2*).

The majority of SCO-active complexes are of iron(II), and most are either monometallic or polymeric (*3*). Dinuclear complexes are less common (*4*), but are particularly appealing owing to the possibility of accessing multiple states in a single molecule, i.e. three-state switching between [HS-HS], '[HS-LS]', and [LS-LS] states. The family of dinuclear iron(II) complexes of the bis-terdentate **PMRT** ligands (Figure 1, box) have been shown to give SCO behaviour (*5–10*), highlights of which include the first structurally (*9*) and Mössbauer spectroscopically (*10*) characterised localised [HS-LS] complex, $[Fe^{II}_2(\mathbf{PMAT})_2](BF_4)_4{\cdot}DMF$ ($T_{½}$ = 224 K), and an intriguing example of scan rate dependent thermal

CONTACT Sally Brooker sbrooker@chemistry.otago.ac.nz
[†]Present address: Department of Chemical and Process Engineering, University of Canterbury, Christchurch 8140, New Zealand.
[‡]Present address: Chemistry, University of Southampton, Southampton SO17 1BJ, England.
[¶]Present address: Bio21 Molecular Science & Biotechnology Institute, School of Chemistry, The University of Melbourne, Parkville, Victoria 3052, Australia.
The supplemental data for this article is available online at https://doi.org/10.1080/10610278.2017.1358449.

hysteresis observed for $[Fe^{II}_2(\mathbf{PMPh^{tBu}T})_2](BF_4)_4{\cdot}3.5H_2O$ (*6*). However, not all **PMRT** complexes are SCO-active; $[Fe^{II}_2(\mathbf{PMPT})_2](BF_4)_4{\cdot}H_2O$ remains [HS-HS] down to 4 K (*5*).

SCO has also been observed for dinuclear complexes of closely-related analogues of the **PMRT** ligands in which either (a) the 1,2,4-triazole ring is replaced by either a thiadazole (*11*) or oxadiazole (*12*) ring, or (b) the secondary amines are replaced by thioethers (**PSRT**) (*13*). Iron(II) complexes of ligands closely related to **PMRT** ligands, but containing a pyrazole ring instead of a 1,2,4-triazole ring, are known but are HS down to 4 K (*14*).

Herein we report another type of analogue of the **PMRT** ligand family, **P$_z$MRT** (Figure 1), which features *pyrazine* rings in place of the pyridine rings (*15*). Pyrazine is a stronger π-acceptor, but weaker σ-donor, than pyridine (*16*). Typically one would anticipate the increase in π-acceptor character to dominate, resulting in a stronger crystal field on the iron(II) centre and stabilisation of the LS state, increasing the $T_{½}$ value. Whilst this is sometimes the case (*17–20*), it is not always observed (Table S1) (*19*, *21–25*). Two possible reasons for this immediately come to mind: either the decrease in σ-donor character has more than offset the increase in π-acceptor character, or crystal packing interactions have obscured the electronic effects. Table S1 (SI) shows some examples of the effect of pyridine vs. pyrazine substitutions on the spin state of iron(II) to illustrate these points.

3,5-Disubstituted-1,2,4-triazole ligands related to the **PMRT** (*5–10*) family, and even more closely to the **Rdpt** family (*19*, *26*) (Figure 1), in which iron(II) complexes of a pair of pyridine and pyrazine analogues were studied, include the pyridine **bpt**H and pyrazine **bpzt**H ligands (Figure 1), reported by Tong et al. (*17*). The resulting $[Fe^{II}(\mathbf{L})_2(AgCN)_2]_n$ (**L** = **bpt**$^-$ or **bpzt**$^-$) complexes adopt one-dimensional chain structures, with the pyridine-containing analogue remaining HS between 4 and 300 K whereas the pyrazine-containing analogue undergoes SCO (with $T_{½}\downarrow$ = 286 and $T_{½}\uparrow$ = 292 K), consistent with pyrazine imparting a stronger ligand field than pyridine. However, in $[Fe^{II}(\mathbf{bpzt})_2(AgCN)_2]_n$ the non-coordinated pyrazine nitrogen atom of **bpzt**$^-$ interacts with the silver ions of adjacent chains, an interaction that cannot be present in $[Fe^{II}(\mathbf{bpt})_2(AgCN)_2]_n$, so clearly the packing effects are not identical for this pair of complexes.

Moving to related, but *neutral*, triazole ligands which bind in a *monotopic* manner, the pyridine-containing complex $[Fe^{II}(\mathbf{\textit{p}\text{-}mdpt})_2(NCS)_2]$ (Figure 1) undergoes SCO with $T_{½}\downarrow$ = 217 and $T_{½}\uparrow$ = 220 K (*27*). When one of the two pyridine rings of ***p*-mdpt** is replaced by pyrazine, giving the ligand **tolpzpy** (Figure 1), one polymorph of the resulting complex $[Fe^{II}(\mathbf{tolpzpy})_2(NCS)_2]$ (Figure 1) showed a spin transition with $T_{½}$ = 145 K, but it is unclear whether the pyridine or pyrazine nitrogen atom is bound to iron(II) (*28*). A different polymorph, where the iron(II) was shown to be bound to the pyridine ring, was HS at all temperatures. When the pyridine ring of **tolpzpy** is replaced with a phenyl ring to ensure that the iron(II) is bound via the pyrazine nitrogen atom (*21*), the resulting complex $[Fe^{II}(\mathbf{tolpzph})_2(NCS)_2]$ (Figure 1) exhibited SCO with $T_{½}$ = 210 K, which is almost identical to when the iron(II) is pyridine-bound in $[Fe^{II}(\mathbf{\textit{p}\text{-}mdpt})_2(NCS)_2]$. So, whilst ***p*-mdpt** and **tolpzph** are *not* direct analogues, as ***p*-mdpt** has a second pyridine ring in the C^5 position whereas **tolpzph** has a phenyl ring, in these complexes the $T_{½}$ is almost unchanged on substituting pyridine for pyrazine.

Other studies have investigated the effect of replacing between one and three of the pyridine rings in terpyridine (**terpy**, Figure 1) with pyrazine (**L^1** to **L^3**, Figure 1). All of the resulting $[Fe^{II}(\mathbf{L})_2](BF_4)_2$ complexes remained LS no matter how many pyridine rings were substituted for pyrazine (*18*). Similar findings were obtained for the related pair of iron(II) complexes of the pyridine-ligand **L^5** vs. pyrazine analogue **py-pzpypz** (Figure 1) (*20*), and for the pair of *tris* complexes, $[Fe^{II}(\mathbf{L})_3](BF_4)_2$, of the bidentate pyrazine **L^7** and pyridine **L^6** ligands (*24*, *29*), all of which are LS.

In contrast, SCO-active iron(II) complexes of tridentate ligands related to **terpy**, 2,6-di(pyrazol-1-yl)*pyridine* (**bpp**, Figure 1) and 2,6-di(pyrazol-1-yl)*pyrazine* (**bppz**, Figure 1), have been widely investigated (*22*, *30*), along with those of substituted derivatives containing additional groups off of the pyrazole (*23*) or pyridine/pyrazine rings (*22*, *30*). In some of the pairs of complexes the *pyrazine analogue gives*

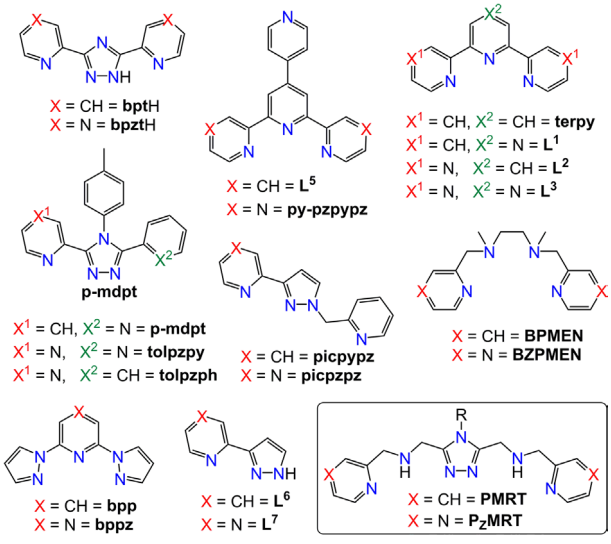

Figure 1. (Colour online) Selected ligands used in pyridine vs. pyrazine ligand field comparisons in the literature in the context of modulating SCO behaviour of iron(II), as well as the **PMRT** vs. **P$_z$MRT** systems (box) compared herein (see Scheme 1).

a stronger ligand field than the pyridine, but in other pairs the reverse is observed. For example, pyridine-based $[Fe^{II}(\mathbf{bpp})_2](ClO_4)_2$ is HS between 5 and 300 K, whereas the pyrazine analogue $[Fe^{II}(\mathbf{bppz})_2](ClO_4)_2$ exhibits SCO with a $T_{½}$ of 201 K, so clearly the LS state is better stabilised by the pyrazine ring (stronger ligand field) in the **bppz** case (*22*). However, for the analogous BF_4^- salts, $[Fe^{II}(\mathbf{bpp})](BF_4)_2$ undergoes SCO at $T_{½}$ = 261 K, whereas $[Fe^{II}(\mathbf{bppz})](BF_4)_2$ displays a transition at $T_{½}$ = 223 K, the opposite trend to that seen for the ClO_4^- salt (*22*). Interestingly, solution-phase measurements on the BF_4^- complexes (in which the effect of crystal packing is removed) show the reverse effect from that seen in the solid state, with the pyrazine complex $[Fe^{II}(\mathbf{bppz})](BF_4)_2$ having a slightly higher $T_{½}$ than for the analogous pyridine complex $[Fe^{II}(\mathbf{bpp})](BF_4)_2$ (Table S1) (*23*, *31*).

Another pair of tridentate ligands, related to bidentate **L⁷**/**L⁶**, but in which the outer pyrazole nitrogen atom possesses a methyl-2-pyridine substituent, **picpypz** and **picpypz** (Figure 1) (*32*), have also been explored as part of a pyridine vs. pyrazine comparison of SCO-active iron(II) complexes. Specifically, pyrazine $[Fe^{II}(\mathbf{picpzpz})](BF_4)_2$·MeOH displays a two-step transition with $T_{½}^{1}$ = 197 K and $T_{½}^{2}$ = 91 K, whereas pyridine $[Fe^{II}(\mathbf{picpypz})](BF_4)_2$·MeOH displays a gradual SCO centred at roughly 225 K (*32*), consistent with *pyridine providing a stronger ligand field than pyrazine*, although clearly other factors are contributing as the transition is single step and gradual rather than abrupt and two-step.

Another study looked at the effect of pyridine vs. pyrazine in the pair of tetradentate ligands **BPMEN** and **BZPMEN** (Figure 1) (*33*). The spin transitions of complexes of the type $[Fe^{II}(\mathbf{L})_2(O_3SCF_3)_2]$ (where **L** = **BZPMEN** or **BPMEN**) were analysed by the Evan's NMR method in acetonitrile-d_6. The pyrazine complex $[Fe^{II}(\mathbf{BZPMEN})_2(O_3SCF_3)_2]$ displayed a higher $T_{½}$ (292 vs. 264 K) than the analogous pyridine complex $[Fe^{II}(\mathbf{BPMEN})_2(O_3SCF_3)_2]$, consistent with *pyrazine providing the stronger ligand field*. Solid-state magnetic measurements were not reported.

Here we probe the effect on the iron(II) spin states of replacing both of the *pyridine* rings in two examples of bis-terdentate **PMRT** ligands with *pyrazine* rings to give the analogous bis-terdentate **P$_z$MRT** ligands (Figure 1).

Results and discussion

Synthesis of ligands

The synthesis of the ligands **P$_z$MAT** and **P$_z$MPT** (Scheme 1) is based on the analogous synthesis of **PMAT** (*7*) and **PMPT** (*5*), except using 2-(aminomethyl)pyrazine instead of commercially available 2-(aminomethyl)pyridine. The 2-(aminomethyl)pyrazine was obtained in five steps. First, picolinic acid was converted to methyl picolinate hydrochloride in 92% yield using thionyl chloride and methanol (avoiding the use of sulphuric acid (*34*)) at room temperature (as is done for related conversions (*35*)), and in a similar fashion to a reported procedure (*36*). The hydrochloride salt is not prone to decomposition like the free base, so is convenient for storage. In the second step, methyl picolinate hydrochloride is converted to the free base, methyl picolinate, in 94% yield using potassium carbonate. The third step is reduction of the ester with sodium borohydride in methanol at room temperature, similar to published procedures at reflux (*37*) but under milder conditions and in higher yield (71%). This reduction has also been reported with lithium borohydride in water (*38*), although the yield was not specified in that case. In the fourth step, a Mitsunobu reaction (using DIAD and triphenylphosphine in dry THF) is employed to convert the alcohol directly to the phthalimide in 75% yield (previously the phthalimide has been obtained by first isolating 2-(chloromethyl)pyrazine (*39*, *40*)). Finally, in the fifth step, the phthalimide group is converted to the amine using hydrazine hydrate in ethanol (*40*), yielding 2-(aminomethyl)pyrazine as a highly hygroscopic pale yellow oil

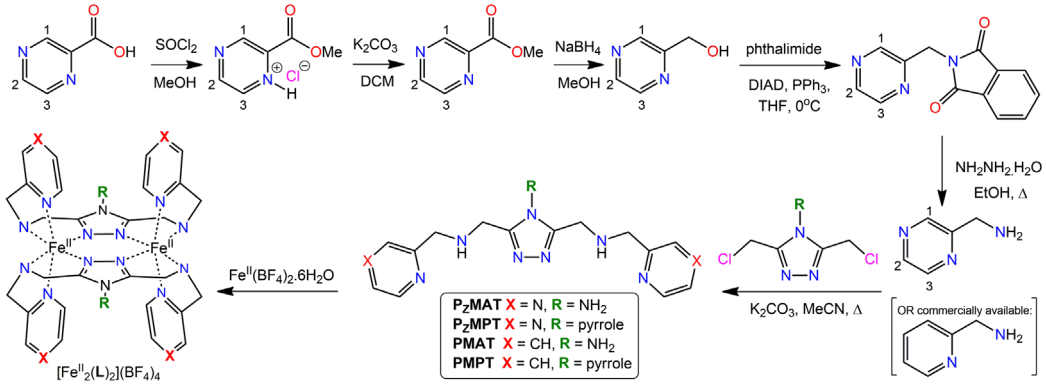

Scheme 1. (Colour online) Preparation of the new pyrazine armed ligands **P$_z$MAT** (R = NH_2) and **P$_z$MPT** (R = pyrrole), and the complexes $[Fe^{II}_2(\mathbf{P_zMRT})_2](BF_4)_4$ and $[Fe^{II}_2(\mathbf{PMRT})_2](BF_4)_4$. The literature ligands **PMAT** and **PMPT** contain pyridine, not pyrazine, rings and are formed from commercially available 2-(aminomethyl)pyridine.

in 74% yield. In the past this conversion was performed using sodium hydroxide (*39*), but this requires laborious extraction of the highly-water soluble amine from water into organic solvents, so the hydrazine hydrate route is far superior.

With this interesting amine in hand, the ligands **P_zMAT** and **P_zMPT** were prepared by refluxing it with either 3,5-bis(chloromethyl)-4-amino-4H-1,2,4-triazole or 3,5-bis(chloromethyl)-4-pyrrole-4H-1,2,4-triazole, respectively, in acetonitrile (Scheme 1). As with the pyridine ligand analogues **PMAT** (*7*) and **PMPT** (*5*), the **P_zMRT** ligands were not purified prior to complexation.

Synthesis of complexes

Analytically pure powders of $[Fe^{II}_2(\mathbf{P_zMAT})_2](BF_4)_4{\cdot}MeOH{\cdot}2H_2O$ (**1**·MeOH·$2H_2O$) and $[Fe^{II}_2(\mathbf{P_zMPT})_2](BF_4)_4{\cdot}3H_2O$ (**2**·$3H_2O$) were obtained by the reaction of $Fe^{II}(BF_4)_2{\cdot}6H_2O$ with an equimolar quantity of **P_zMAT** or **P_zMPT**, respectively, in methanol using Schlenk techniques (Scheme 1). It should be noted that all subsequent analyses, including magnetic studies, were performed on these powder samples.

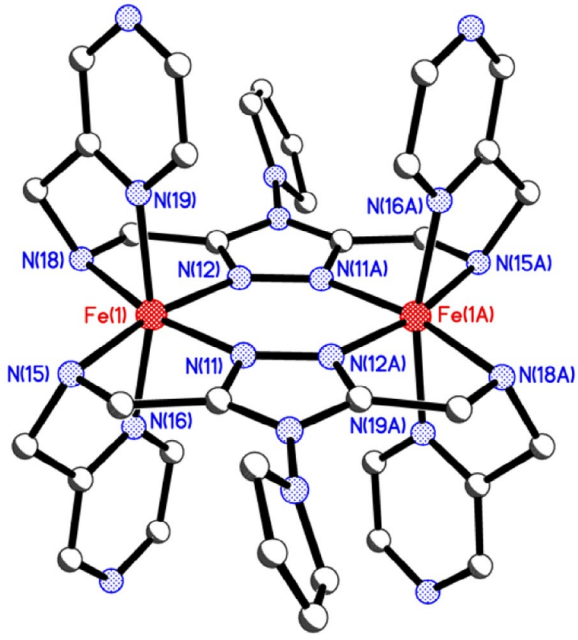

Figure 2. (Colour online) Perspective view of the one of the two unique complexes in the crystal structure of $[Fe^{II}_2(\mathbf{P_zMPT})_2](BF_4)_4{\cdot}3.5MeCN$ (**2**·3.5MeCN). For clarity, hydrogen atoms and solvent molecules have been omitted.

Crystal structure

Despite numerous attempts, crystals of **1** were not obtained. However, a few single crystals of **2**·3.5MeCN, suitable for X-ray diffraction, were grown by slow diffusion of diethyl vapour into a solution of **2**·$3H_2O$ in acetonitrile. The complex crystallised in the triclinic space-group P-1 with the asymmetric unit composed of two half-complexes, four tetrafluoroborate anions and three and a half acetonitrile molecules, with the remainder of each complex generated by inversion (Figure 2 and S1, Table 1 and S2, SI).

The two independent complexes are very similar to one another [Table 1, Fe(1) vs. Fe(2)]. In both cases the $[Fe^{II}_2(\mathbf{P_zMPT})_2]^{4+}$ cation comprises two iron(II) centres coordinated in a *cis*-axial (*13*) fashion by two **P_zMPT** ligands. Overall this is very similar to that of the pyridyl-armed analogue $[Fe^{II}_2(\mathbf{PMPT})_2](BF_4)_4{\cdot}4DMF$ (*5*). The iron(II) centres in **2**·3.5MeCN at 100 K have shorter Fe–N bonds and smaller Σ values (*41*) compared to related [HS-HS] $[Fe^{II}_2(\mathbf{PMRT})_2](BF_4)_2$ complexes, but longer than for the related localised [LS-HS] complex (Table 1) (*5–10*). Indeed the average Fe–N in **2**·3.5MeCN lies between that seen for LS and HS iron(II) in related ligands, and consistent with an average occupancy of 2:1 HS:LS at each iron(II) site. Given that no $[Fe^{II}(\mathbf{PMRT})_2](BF_4)_2$ complex has been observed in the fully [LS-LS] state, it is likely that this is a consequence of a disordered 1:2 mixture of [HS-HS] and '[HS-LS]' throughout the crystal lattice.

Analysis of the packing interactions reveals hydrogen bonds between three of the unique secondary amine protons and the fluorine atoms of nearby tetrafluoroborate counter anions (N–H···F = 2.891–3.168 Å, $\angle_{N-H\cdots F}$ = 151.4–163.7°), with the fourth amine proton forming a weak bifurcated hydrogen bond to the nitrogen atom of a lattice

Table 1. Comparison of selected structural parameters of $[Fe^{II}_2(\mathbf{P_zMPT})_2](BF_4)_4{\cdot}3.5MeCN$ (**2**·3.5MeCN) (two half-complexes in the asymmetric unit) with $[Fe^{II}_2(\mathbf{PMPT})_2](BF_4)_4{\cdot}4DMF$ and $[Fe^{II}_2(\mathbf{PMAT})_2](BF_4)_4{\cdot}DMF$ (in both its [HS-HS] and localised [LS-HS] states).

	Fe(1) complex 1 **2**·3.5MeCN	Fe(2) complex 2 **2**·3.5MeCN	Fe(1) in $[Fe^{II}_2(\mathbf{PMPT})_2](BF_4)_4{\cdot}4DMF$[5]	Fe(1) in $[Fe^{II}_2(\mathbf{PMAT})_2](BF_4)_4{\cdot}DMF$[9]	Fe(1) vs Fe(2) in $[Fe^{II}_2(\mathbf{PMAT})_2](BF_4)_4{\cdot}DMF$[9]
Temperature (K)	100	100	100	298	123
Spin state	Average of 2:1 HS:LS	Average of 2:1 HS:LS	HS-HS	HS-HS	LS-HS
Fe-$N_{triazole}$ (Å)	2.065(6),2.066(6)	2.047(6),2.058(7)	2.102(2),2.128(2)	2.116(4),2.123(4)	1.934(3), 1.946(3) 2.131(3), 2.136(3)
Fe-N_{amine} (Å)	2.199(7),2.203(7)	2.218(6),2.224(7)	2.334(2),2.304(2)	2.289(5),2.303(5)	2.066(4), 2.071(4) 2.312(4), 2.319(4)
Fe-$N_{pyrazine}$ (Å)	2.061(7),2.073(7)	2.072(6),2.081(6)	2.137(2),2.125(2)	2.147(5),2.148(4)	1.986(4), 1.987(4) 2.155(4), 2.159(4)
Average Fe-N (Å)	2.110	2.118	2.188	2.186	1.998 2.202
Σ (°)	97.4	102.9	119.9	117.5	64.92 133.15

acetonitrile molecule (N–H···N = 3.287, $\angle_{N-H\cdots N}$ = 132.9°) and a non-coordinated pyrazine nitrogen atom (N–H···N = 3.484 Å, $\angle_{N-H\cdots N}$ = 138.1°). The other three unique non-coordinated pyrazine nitrogen atoms are involved in non-classical hydrogen bonds with the protons on the sp^3 carbon atoms of lattice acetonitrile molecules (C–H···N = 2.960–3.292 Å, $\angle_{C-H\cdots N}$ = 132.94–130.55°). There are also anion–π interactions (*42*) (F11···centroid of pyrazine ring = 3.118 Å). In contrast, in the structure of $[Fe^{II}_2(\mathbf{PMPT})_2](BF_4)_4$·4DMF all four secondary amine protons are hydrogen bonding to fluorine atoms of counter anions, and the solvent DMF molecules interact with the complex cation via O–H···π interactions (*5*) rather than via the non-coordinated pyrazine nitrogen atoms. Nevertheless, anion–π interactions are observed in both cases.

Magnetic and Mössbauer study

The magnetic properties of **1**·MeOH·$2H_2O$ and **2**·$3H_2O$ were measured between 300 and 4 K to check for the presence of SCO (Figure 3 and Table 2). At room temperature, the χT product *per iron(II)* for **1**·MeOH·$2H_2O$ is 2.32 cm^3·K·mol^{-1} (4.31 B.M.) and for **2**·$3H_2O$ it is slightly higher, 2.58 cm^3·K·mol^{-1} (4.55 B.M.). Assuming a χT product of 3.51 cm^3·K·mol^{-1} for HS iron(II) (*43*), these correspond to about two-thirds to three-quarters of the iron(II) ions being in the high-spin state. As the temperature is lowered to 50 K, there is an incomplete and gradual SCO, as evidenced by a decrease in the χT product to 1.57 and 1.77 cm^3·K·mol^{-1} per iron(II) for **1**·MeOH·$2H_2O$ and **2**·$3H_2O$, respectively. Both of these values are in the range expected for half of the iron(II) ions being in the HS state, i.e. a '[HS-LS]' state, at 50 K.

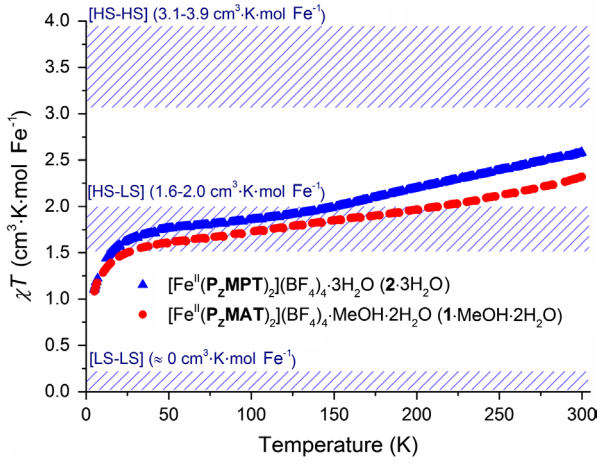

Figure 3. (Colour online) Temperature dependence of the χT product for **1**·MeOH·$2H_2O$ (blue points) and **2**·$3H_2O$ (red points) between 300 and 4 K, collected in the sweep mode at 5 K·min^{-1}.

Table 2. Comparison of the χT product per Fe (cm^3·K·mol^{-1}) for pyrazine complexes **1**·MeOH·$2H_2O$ and **2**·$3H_2O$ (powders) with the pyridine-containing analogues $[Fe^{II}_2(\mathbf{PMAT})_2](BF_4)_4$·DMF and $[Fe^{II}_2(\mathbf{PMPT})_2](BF_4)_4$·$H_2O$ (crystalline).

	χT at 50 K	χT at 300 K
$[Fe^{II}_2(\mathbf{P_zMAT})_2](BF_4)_4$·MeOH·$2H_2O$ (**1**·MeOH·$2H_2O$)	1.57	2.32
$[Fe^{II}_2(\mathbf{PMAT})_2](BF_4)_4$·DMF (*7–10*)	1.88	3.44
$[Fe^{II}_2(\mathbf{P_zMPT})_2](BF_4)_4$·$3H_2O$ (**2**·$3H_2O$)	1.77	2.58
$[Fe^{II}_2(\mathbf{PMPT})_2](BF_4)_4$·$H_2O$ (*5*)	2.91	2.91

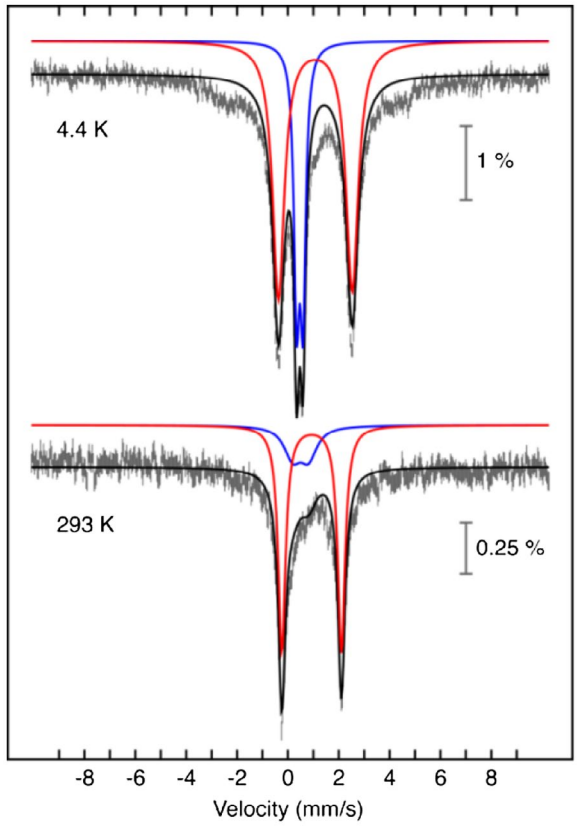

Figure 4. (Colour online) The Mössbauer spectrum of **2**·H_2O at 4.4 K (top) and 293 K (bottom). The solid coloured lines are a fit, and correspond to HS (red) and LS (blue) iron(II).

Whilst the analogous pyridyl-containing complexes $[Fe^{II}_2(\mathbf{PMAT})_2](BF_4)_4$·DMF and $[Fe^{II}_2(\mathbf{PMPT})_2](BF_4)_4$·$H_2O$ (Table 2) are both fully [HS-HS] at room temperature, both **1**·MeOH·$2H_2O$ and **2**·$3H_2O$ are already partially LS, *consistent with pyrazine providing a somewhat stronger ligand field than pyridine*. However, both pyrazine samples are powders, and undergo very gradual SCO, whereas crystals of $[Fe^{II}_2(\mathbf{PMAT})_2](BF_4)_4$·DMF undergo an abrupt 'half' SCO from [HS-HS] to a localised [HS-LS] state (i.e. one HS and one LS centre within the same molecule) with $T_{½}$ = 224 K (*7–10*), and a powder sample of $[Fe^{II}_2(\mathbf{PMPT})_2](BF_4)_4$·$H_2O$ remains [HS-HS] at all temperatures studied (*5*).

The Mössbauer spectrum of solvatomorph **2**·H_2O at 4.4 K (Figure 4 and Table S3, SI) shows two signals; a wider

doublet at isomer shift δ = 1.08 with quadrupole splitting ΔE_Q = 2.90 mm·s^{-1} corresponding to HS iron(II), and a narrow doublet at δ = 0.47 with quadrupole splitting ΔE_Q = 0.25 mm·s^{-1} corresponding to LS iron(II). There is an additional broad background signal which is probably due to some oxidation that these complexes are prone to. The relative intensity of the HS:LS peaks, 2:1, corresponds to a χT product of approximately 2.3 cm^3·K·mol^{-1}, which is somewhat higher than the value derived from the magnetic data at 50 K (1.77 cm^3·K·mol^{-1}).

At 293 K, the isomer shifts (0.94 for HS, 0.50 mm·s^{-1} LS) and quadrupole splittings (2.34 for HS; 0.62 mm·s^{-1} for LS) are relatively unchanged from those at 4.4 K. However, the relative intensity of the peaks has changed to 3:1 HS:LS, which corresponds $\chi T \approx$2.6 cm^3·K·mol^{-1}. This is in very good agreement with that obtained from the magnetic measurements (2.58 cm^3·K·mol^{-1}). Whilst the parameters are very similar to those found in the Mössbauer spectra of [Fe$^{II}_2$(**PMAT**)$_2$](BF$_4$)$_4$·DMF (*10*) and [Fe$^{II}_2$(**PMPh^{tBu}T**)$_2$](BF$_4$)$_4$·3.5H$_2$O (*6*), the present data cannot distinguish between a delocalised [HS-LS] state or a mixture of [HS-HS] and [LS-LS] states at 4.4 K for **2**·H$_2$O.

Conclusion

The *pyrazine* analogues, [Fe$^{II}_2$(**P$_Z$MAT**)$_2$](BF$_4$)$_4$·MeOH·2H$_2$O (**1**·MeOH·2H$_2$O) and [Fe$^{II}_2$(**P$_Z$MPT**)$_2$](BF$_4$)$_4$·3H$_2$O (**2**·3H$_2$O), of the previously reported *pyridine* complexes [Fe$^{II}_2$(**PMAT**)$_2$](BF$_4$)$_4$·DMF and [Fe$^{II}_2$(**PMRT**)$_2$](BF$_4$)$_4$·H$_2$O, have been prepared and characterised. The structure determination on **2**·3.5MeCN confirmed the expected binding mode, with two bis-terdentate ligands providing all 12 donors to the two iron(II) centres as well as two triazole bridges between them. In contrast to the pyridine analogues, neither pyrazine complex is fully [HS-HS] at room temperature, consistent with *pyrazine providing a stronger ligand field than pyridine*. Also consistent with this is that whilst [Fe$^{II}_2$(**PMRT**)$_2$](BF$_4$)$_4$·H$_2$O remains [HS-HS], both **1**·MeOH·2H$_2$O and **2**·3H$_2$O show very gradual SCO, to approximately '[HS-LS]' at 50 K. However, these comparisons must be taken on board with caution, as the solvent content varies, as does the crystalline vs. powder nature of these samples, factors which are known to have the potential to confound. These systems have proved to be oxidation sensitive, so our focus is now on more robust systems with which we can examine the relative field strengths of pyridine and pyrazine in more detail.

Experimental

General remarks

The synthesis of 3,5-bis(chloromethyl)-4-amino-1,2,4-triazole and 3,5-bis(chloromethyl)-4-pyrrole-1,2,4-triazole has been previously reported (*9*). All other materials were purchased from commercial suppliers and used as received. Elemental analysis was carried out by the Campbell Microanalytical Laboratory at the University of Otago. ^{1}H NMR spectra were recorded on a 400 MHz Varian 400MR spectrometer at 298 K. Chemical shifts are referenced to residual solvent peaks ($CDCl_3$ at 7.26 ppm).

Magnetic data were recorded over the range 4–300 K using a Quantum Design PPMS Susceptometer equipped with a vibrating sample mount or a Quantum Design SQUID Magnetometer under an applied field of 0.1 Tesla at the Robinson Research Institute, Lower Hutt, New Zealand. ^{57}Fe Mössbauer spectroscopy were recorded on a Mössbauer spectrometer from SEE Co. equipped with a closed cycle refrigerator system from Janis Research Co. and SHI. Data were collected in constant acceleration mode in transmission geometry with an applied field of 47 mT parallel to the γ-rays. The zero velocity of the Mössbauer spectra refers to the centroid of the room temperature spectrum of a 25 μm metallic iron foil. Analysis of the spectra was conducted using the WMOSS program (SEE Co., formerly WEB Research Co. Edina, MN).

Single crystal X-ray diffraction data for all complexes were collected on a Bruker Kappa Apex II area detector diffractometer at 91 K. In all cases graphite monochromated Mo-K$_\alpha$ radiation (λ = 0.71073 Å) was used. All data sets were corrected for absorption using SCALE (*44*). The structures were solved using SHELXS-97 (*45*). All structures were refined against F^2 using all data by full matrix least squares techniques with SHELXL-97 (*45*). Crystallographic data for the structure of **2**·3.5MeCN has been deposited with the Cambridge Crystallographic Data Centre, CCDC 1552217. Further refinement details are available in the ESI.

Synthesis

Methyl 2-pyrazinecarboxylate hydrochloride: 2-Pyrazinecarboxylic acid (75 g, 0.605 mol) was suspended in methanol (500 mL) and thionylchloride (44.0 mL, 0.605 mol) was slowly added with stirring. The suspension was stirred for two days before being filtered and the solid suspended in diethyl ether (750 mL). The suspension was filtered and the solid washed with diethyl ether to yield crude product as a flowing white powder (97 g, 92%). Found: C 41.95, H 4.05, N 16.86. Calc. for C$_6$H$_6$N$_2$O$_2$·HCl: C, 41.91, H, 4.05, N, 16.05. ^{1}H NMR (300 MHz, $CDCl_3$): δ (ppm) 9.34 (d, J = 1.5 Hz, 1H, H-3), 8.79 (d, J = 2.7 Hz, 1H, H-1), 8.75–8.74 (m, 1H, H-2), 4.07 (s, 3H, OCH$_3$).

Methyl 2-pyrazinecarboxylate: To a stirred suspension of methyl 2-pyrazinecarboxylate hydrochloride (49.6 g, 0.284 mol) in dichloromethane (300 mL) was added potassium carbonate (48.6 g, 0.352 mol) and the suspension was stirred for five hours, during which time the suspended

solid became flocculent. The suspension was then filtered and the filtrate evaporated to dryness under reduced pressure at 40 °C to yield methyl 2-pyrazinecarboxylate as colourless oil which rapidly crystallised into an off-white solid at room temperature (37.0 g, 94%). Found: C, 51.94; H, 4.55; N, 20.55. Calc. for $C_6H_6N_2O_2$: C, 52.17; H, 4.38; N, 20.28. 1H NMR (300 MHz, $CDCl_3$): δ (ppm) 9.33 (d, J = 1.0 Hz, 1H, H-3), 8.79 (d, J = 2 Hz, 1H, H-1), 8.74–8.73 (m, 1H, H-2), 4.06 (s, 3H, OCH_3).

2-Pyrazinemethanol: A stirred solution of methyl 2-pyrazinecarboxylate (4.94 g, 35.8 mmol) in methanol (350 mL) was slowly added sodium borohydride (5.410 g, 143 mmol) in 1 g portions over 10 min. Caution: The solution became yellow and evolved heat and gas, add the sodium borohydride cautiously. The solution was stirred overnight at room temperature. H_2O (20 mL) was added and the reaction was shaken vigorously. The suspension was then evaporated to dryness under reduced pressure to an oily yellow powder. Ethyl acetate (350 mL) was then added and the resulting suspension was stirred vigorously overnight. The suspension was filtered and evaporated to dryness under vacuum to give the crude product as a yellow oil which was used without further purification (2.80 g, ca. 71%). ^{1}H NMR (300 MHz, $CDCl_3$): δ (ppm) 8.64 (br, 1H, H-3), 8.53 (m, 1H, H-2), 8.50 (m, 1H, H-1), 4.84 (s, 2H, CH_2).

2-Pyrazinemethylphthalimide: Triphenylphosphine (7.80 g, 29.7 mmol) and phthalimide (4.50 g, 30.6 mmol) were added to a solution of crude 2-(hydroxylmethyl)pyrazine (2.80 g, 25.5 mmol) in dry tetrahydrofuran (200 mL). The stirred solution was then cooled in an ice bath before diisopropyl azodicarboxylate (5.90 g, 30.4 mmol) was slowly added over 5 min. The solution was stirred for two days at room temperature and taken to dryness under reduced pressure and the resulting yellow oil was suspended in ethanol (20 mL) before again being taken to dryness under reduced pressure, producing a thick yellow slurry. The slurry was dissolved in hot ethanol (~200 mL) and left to cool and evaporate to ~50 mL overnight at room temperature. The resulting solid was filtered off to give the desired product as an analytically pure slightly yellow solid (3.82 g, 75%). Found: C, 65.14; H, 3.89; N, 17.52. Calc. for $C_{13}H_9N_3O_2$: C, 65.27; H, 3.79; N, 17.56. ^{1}H NMR (300 MHz, $CDCl_3$): δ (ppm) 8.66 (s, 1H, H-3), 8.48 (s, 2H, H-2 + H-1), 7.89–7.92 (m, 2H, phth-H), 7.77–7.74 (m, 2H, phth-H), 5.06 (s, 2H, CH_2).

2-(Aminomethyl)pyrazine: 2-Pyrazinemethylphthalimide (0.15 g, 0.63 mmol) was suspended in ethanol (10 mL) and hydrazine hydrate (80% w/w%, 1.5 mL, 3.1 mmol) added before the suspension was heated to reflux for two hours. The suspension was then cooled to room temperature then further cooled in the fridge. The suspension was filtered and the filtrate taken to dryness yielding 2-(aminomethyl)pyrazine as a yellow oil that was used without further purification (0.05 g, ca. 74%). Found: C, 52.70; H, 6.60; N, 36.43. Calculated for $C_5H_7N_3O$·⅓H2O: C, 52.43; H, 6.69; N, 36.69. ^{1}H NMR (300 MHz, $CDCl_3$): δ (ppm) 8.54 (d, J = 1.5 Hz, 1H, H-3), 8.46 (dd, J = 1.5, 2.7 Hz, 1H, H-2), 8.40 (d, $J_{1,2}$ = 2.7 Hz, 1H, H-1), 3.96 (s, 2H, CH_2).

3,5-Bis{[(2-pyrazylmethyl)amino]methyl}-4-amino-4H-1,2,4-triazole (**P_zMAT**): 2-(aminomethyl)pyrazine (0.5 g, 4.58 mmol) and 3,5-bis(chloromethyl)-4-amino-1,2,4-triazole (0.331 g, 1.53 mmol) were dissolved in acetonitrile (40 mL). To this was added K_2CO_3 (1.05 g, 7.64 mmol) and the resulting suspension heated at reflux for four hours. At this point the suspension was filtered and the filtrate taken to dryness. The residue was dissolved in dichloromethane (10 mL) and the white solid (residual Na_2CO_3) filtered off. The filtrate was taken to dryness, yielding crude 3,5-bis{[(2-pyrazylmethyl)amino]methyl}-4-amino-4H-1,2,4-triazole (**P_zMAT**) as a red oil. The ligand was used as is, without further purification.

3,5-Bis{[(2-pyrazylmethyl)amino]methyl}-4-pyrrole-4H-1,2,4-triazole (**P_zMPT**): Prepared in an analogous fashion to **P_zMAT**, except using 3,5-bis(chloromethyl)-4-*pyrrole*-1,2,4-triazole (0.293 g, 1.53 mmol), with the same quantities of other reagents and solvents, yielding red oil. The ligand was used as is, without further purification.

$[Fe^{II}_2(\mathbf{P_zMAT})_2](BF_4)_4$·MeOH·$2H_2O$ (**1**·MeOH·$2H_2O$): 3,5-bis{[(2-pyrazylmethyl)amino]methyl}-4-amino-4H-1,2,4-triazole (0.216 g, 0.69 mmol) was dissolved in MeOH (5 mL) and the solution thoroughly degassed by consecutive vacuum/argon purges. To MeOH (5 mL) degassed by consecutive vacuum/argon purges was added $Fe^{II}(BF_4)_2$·$6H_2O$ (0.222 g, 0.69 mmol) and the solution transferred via cannula to the **P_zMAT** solution. The resulting brown suspension was stirred for a further five minutes before being filtered under argon yielding $[Fe^{II}_2(\mathbf{P_zMAT})_2](BF_4)_4$·$2H_2O$·MeOH as brown powder (0.190 g, 49%). Found: C, 29.29; H, 3.36; N, 23.76. Calc. for $Fe_2C_{28}H_{36}N_{20}B_4F_{16}$·$2H_2O$·MeOH: C, 29.53; H, 3.76; N, 23.75. ESI-MS (MeCN): found = 327.1789, calculated for $[(C_{14}H_{18}N_{10})H]^+$ = 327.1794.

$[Fe^{II}_2(\mathbf{P_zMPT})_2](BF_4)_4$·$3H_2O$ (**2**·$3H_2O$): Prepared in analogous fashion to $[Fe^{II}_2(\mathbf{P_zMAT})_2](BF_4)_4$·MeOH·$2H_2O$, except using **$P_z$MPT** (0.240 g, 0.71 mmol), with the same quantities of other reagents and solvents, yielding orange powder (0.292 g, 83%). Found: C, 33.90; H, 3.56; N, 21.75. Calc. for $Fe_2C_{36}H_{40}N_{20}B_4F_{16}$·$3H_2O$: C, 34.16; H, 3.66; N, 22.13. ESI-MS (MeCN): found = 377.1996, calculated for $[(C_{18}H_{20}N_{10})H]^+$ = 377.1951.

Acknowledgements

We thank Dr. Shen Chong and Dr. Simon Granville (Robinson Research Institute) for their assistance with the SQUID magnetometer and PPMS susceptometer.

Disclosure statement

No potential conflict of interest was reported by the authors.

Funding

This work was supported by funding from the University of Otago (including PhD scholarships for HLCF and MGC); the Marsden Fund (RSNZ; including postdoctoral fellowships to JAK and HLCF); the MacDiarmid Institute for Advanced Materials and Nanotechnology.

References

(1) Gütlich, P.; Goodwin, H.A. *Top. Curr. Chem.* **2004**, *233*, 1–47; Gütlich, P.; Gaspar, A.B.; Garcia, Y. *Beilstein J. Org. Chem.* **2013**, *9*, 342–391; Halcrow, M.A. *Spin-crossover Materials: Properties and Applications*, 1st ed.; John Wiley & Sons Ltd: Chichester, **2013**; Brooker, S. *Chem. Soc. Rev.* **2015**, *44*, 2880–2892 and front cover feature.

(2) Senthil Kumar, K.; Ruben, M. *Coord. Chem. Rev.* **2017**. doi:10.1016/j.ccr.2017.1003.1024; Gaspar, A.B.; Seredyuk, M. *Coord. Chem. Rev.* **2014**, *268*, 41–58; Sy, M.; Varret, F.; Boukheddaden, K.; Bouchez, G.; Marrot, J.; Kawata, S.; Kaizaki, S. *Angew. Chem. Int. Ed.* **2014**, *53*, 7539–7542; Coronado, E.; Minguez Espallargas, G. *Chem. Soc. Rev.* **2013**, *42*, 1525–1539; Shepherd, H.J.; Gural'skiy, I.A.; Quintero, C.M.; Tricard, S.; Salmon, L.; Molnár, G.; Bousseksou, A. *Nat. Commun.* **2013**, *4*, 2607; Schafer, B.; Rajnak, C.; Salitros, I.; Fuhr, O.; Klar, D.; Schmitz-Antoniak, C.; Weschke, E.; Wende, H.; Ruben, M. *Chem. Commun.* **2013**, *49*, 10986–10988; Roubeau, O. *Chem. Eur. J.* **2012**, *18*, 15230–15244; Muñoz-Lara, F.J.; Gaspar, A.B.; Muñoz, M.C.; Lysenko, A.B.; Domasevitch, K.V.; Real, J.A. *Inorg. Chem.* **2012**, *51*, 13078–13080; Cavallini, M.; Bergenti, I.; Milita, S.; Kengne, J.C.; Gentili, D.; Ruani, G.; Salitros, I.; Meded, V.; Ruben, M. *Langmuir* **2011**, *27*, 4076–4081; Raza, Y.; Volatron, F.; Moldovan, S.; Ersen, O.; Huc, V.; Martini, C.; Brisset, F.; Gloter, A.; Stephan, O.; Bousseksou, A.; Catala, L.; Mallah, T. *Chem. Commun.* **2011**, *47*, 11501–11503; Halcrow, M.A. *Chem. Soc. Rev.* **2011**, *40*, 4119–4142; Bousseksou, A.; Molnár, G.; Salmon, L.; Nicolazzi, W. *Chem. Soc. Rev.* **2011**, *40*, 3313–3335; Cobo, S.; Molnár, G.; Real, J.A.; Bousseksou, A. *Angew. Chem. Int. Ed.* **2006**, *45*, 5786–5789; Murray, K.S.; Kepert, C.J. *Top. Curr. Chem.* **2004**, *233*, 195–228; Létard, J.-F.; Guionneau, P.; Goux-Capes, L. *Top. Curr. Chem.* **2004**, *235*, 221–249.

(3) Olguín, J.; Brooker, S. In *Spin-crossover Materials: Properties and Applications*, 1st ed.; Halcrow, M.A., Ed.; John Wiley & Sons: Chichester, UK, **2013**; pp 77–120; Murray, K.S. *Eur. J. Inorg. Chem.* **2008**, *20*, 3101–3121.

(4) Schneider, C.J.; Cashion, J.D.; Chilton, N.F.; Etrillard, C.; Fuentealba, M.; Howard, J.A.K.; Létard, J.-F.; Milsmann, C.; Moubaraki, B.; Sparkes, H.A.; Batten, S.R.; Murray, K.S. *Eur. J. Inorg. Chem.* **2013**, *2013*, 850–864.

(5) Kitchen, J.A.; Olguín, J.; Kulmaczewski, R.; White, N.G.; Milway, V.A.; Jameson, G.N.L.; Tallon, J.L.; Brooker, S. *Inorg. Chem.* **2013**, *52*, 11185–11199.

(6) Kulmaczewski, R.; Olguín, J.; Kitchen, J.A.; Feltham, H.L.C.; Jameson, G.N.L.; Tallon, J.L.; Brooker, S. *J. Am. Chem. Soc.* **2014**, *136*, 878–881.

(7) Kitchen, J.A.; White, N.G.; Jameson, G.N.L.; Tallon, J.L.; Brooker, S. *Inorg. Chem.* **2011**, *50*, 4586–4597.

(8) Bhattacharjee, A.; Ksenofontov, V.; Kitchen, J.A.; White, N.G.; Brooker, S.; Gütlich, P. *Appl. Phys. Lett.* **2008**, *92*, 174104; Bhattacharjee, A.; Roy, M.; Ksenofontov, V.; Kitchen, J.A.; Brooker, S.; Gütlich, P. *Eur. J. Inorg. Chem.* **2013**, 843–849.

(9) Klingele, M.H.; Moubaraki, B.; Cashion, J.D.; Murray, K.S.; Brooker, S. *Chem. Commun.* **2005**, *10*, 987–989 and front cover feature.; Klingele, M.H.; Moubaraki, B.; Murray, K.S.; Brooker, S. *Chem. Eur. J.* **2005**, *11*, 6962–6973.

(10) Grunert, C.M.; Reiman, S.; Spiering, H.; Kitchen, J.A.; Brooker, S.; Gütlich, P. *Angew. Chem. Int. Ed.* **2008**, *47*, 2997–2999 and front cover feature.

(11) Herold, C.F.; Shylin, S.I.; Rentschler, E. *Inorg. Chem.* **2016**, *55*, 6414–6419; Herold, C.F.; Carrella, L.M.; Rentschler, E. *Eur. J. Inorg. Chem.* **2015**, *2015*, 3632–3636.

(12) Köhler, C.; Rentschler, E. *Eur. J. Inorg. Chem.* **2016**, *2016*, 1955–1960.

(13) Hogue, R.W.; Feltham, H.L.C.; Miller, R.G.; Brooker, S. *Inorg. Chem.* **2016**, *55*, 4152–4165.

(14) Noble, A.; Olguîn, J.; Clérac, R.; Brooker, S. *Inorg. Chem.* **2010**, *49*, 4560–4569; Olguín, J.; Jameson, G.N.L.; Brooker, S. *Dalton Trans.* **2011**, *40*, 5086–5089; Ng, G.K.Y.; Ziller, J.W.; Borovik, A.S. *Inorg. Chem.* **2011**, *50*, 7922–7924.

(15) Olguín, J.; Brooker, S. *Coord. Chem. Rev.* **2011**, *255*, 203–240.

(16) Steel, P.J. *Coord. Chem. Rev.* **1990**, *106*, 227–265; Wilberg, K.B.; Nakaji, D.; Breneman, C.M. *J. Am. Chem. Soc.* **1989**, *111*, 4178–4190.

(17) Yan, Z.; Li, J.-Y.; Liu, T.; Ni, Z.-P.; Chen, Y.-C.; Guo, F.-S.; Tong, M.-L. *Inorg. Chem.* **2014**, *53*, 8129–8135.

(18) Kershaw Cook, L.J.; Tuna, F.; Halcrow, M.A. *Dalton Trans.* **2013**, *42*, 2254–2265.

(19) Feltham, H.L.C.; Barltrop, A.S.; Brooker, S. *Coord. Chem. Rev.* **2017**, *344*, 26–53.

(20) Miller, R.G.; Brooker, S. *Inorg. Chem.* **2015**, *54*, 5398–5409; Constable, E.C.; Thompson, A.M.W.C. *J. Chem. Soc. Dalton Trans.* **1992**, 2947–2950.

(21) Miller, R.G.; Brooker, S. *Chem. Sci.* **2016**, *7*, 2501–2505 and front cover feature.

(22) Halcrow, M.A. *Coord. Chem. Rev.* **2009**, *253*, 2493–2514.

(23) Mohammed, R.; Chastanet, G.; Tuna, F.; Malkin, T.L.; Barrett, S.A.; Kilner, C.A.; Létard, J.-F.; Halcrow, M.A. *Eur. J. Inorg. Chem.* **2013**, *2013*, 819–831.

(24) Smithson, R.J.; Kilner, C.A.; Brough, A.R.; Halcrow, M.A. *Polyhedron* **2003**, *22*, 725–733.

(25) Leita, B.A.; Neville, S.M.; Halder, G.J.; Moubaraki, B.; Kepert, C.J.; Létard, J.-F.; Murray, K.S. *Inorg. Chem.* **2007**, *46*, 8784–8795.

(26) Kitchen, J.A.; Brooker, S. *Coord. Chem. Rev.* **2008**, *252*, 2072–2092.

(27) Shen, G.-P.; Qi, L.; Wang, L.; Xu, Y.; Jiang, J.-J.; Zhu, D.; Liu, X.-Q.; You, X. *Dalton Trans.* **2013**, *42*, 10144–10152.

(28) Hogue, R.W.; Miller, R.G.; White, N.G.; Feltham, H.L.C.; Jameson, G.N.L.; Brooker, S. *Chem. Commun.* **2014**, *50*, 1435–1437.

(29) Sugiyarto, K.H.; Goodwin, H.A. *Aust. J. Chem.* **1988**, *41*, 1645–1663.

(30) Halcrow, M.A. *Coord. Chem. Rev.* **2005**, *249*, 2880–2908; Kershaw Cook, L.J.; Mohammed, R.; Sherborne, G.; Roberts, T.D.; Alvarez, S.; Halcrow, M.A. *Coord. Chem. Rev.* **2015**, *289*, 2–12.

(31) Holland, J.M.; McAllister, J.A.; Kilner, C.A.; Thornton-Pett, M.; Bridgeman, A.J.; Halcrow, M.A. *J. Chem. Soc. Dalton Trans.* 2002, 548–554.
(32) Leita, B.A.; Neville, S.M.; Halder, G.J.; Moubaraki, B.; Kepert, C.J.; Létard, J.-F.; Murray, K.S. *Inorg. Chem.* **2007**, *46*, 8784–8795.
(33) England, J.; Gondhia, R.; Bigorra-Lopez, L.; Petersen, A.R.; White, A.J.P.; Britovsek, G.J.P. *Dalton Trans.* **2009**, *220*, 5319–5334.
(34) Lee, Y.H.; Lee, J.M.; Kim, S.G.; Lee, Y.S. *Bioorg. Med. Chem.* **2016**, *24*, 2843–2851.
(35) Brooker, S.; Dunbar, G.S.; Jameson, G.B. *Polyhedron* **1999**, *18*, 679–688.
(36) Vergara, F.M.F.; da S. Lima, C.H.; de O. Henriques, M.d.G.M.; Candéa, A.L.P.; Lourenço, M.C.S.; de L. Ferreira, M.; Kaiser, C.R.; de Souza, M.V.N. *Eur. J. Med. Chem.* **2009**, *44*, 4954–4959.
(37) Boechat, N.; da Costa, J.; Mendonca, J.; Paes, K.C.; Fernandes, E.L.; De Oliviera, P.S.M.; Vasconcelos, T.R.A.; de Souza, M.V.N. *Synth. Commun.* **2005**, *35*, 3187–3190; Branytska, O.; Shimon, L.J.W.; Neumann, R. *Chem. Commun.* **2007**, 3957–3959.
(38) Gonzalez-de-Castro, A.; Robertson, C.M.; Xiao, J. *J. Am. Chem. Soc.* **2014**, *136*, 8350–8360.
(39) Hirschberg, A.; Mattner, P.G. *J Med. Chem.* **1968**, *11*, 911–912.
(40) Huang, W.-J.; Hu, M.-H.; Li, J.-M.; Ye, W.-F.; Zhu, X.-Y. *Huaxue Shiji* **2014**, *36*, 599–602.
(41) Guionneau, P.; Brigouleix, C.; Barrans, Y.; Goeta, A.E.; Létard, J.-F.; Howard, J.A.K.; Gaultier, J.; Chasseau, D. *Comptes Rendus Acad. Sci. Ser. Ilc* **2001**, *4*, 161–171; Deeney, F.A.; Charles, J.H.; Morgan, G.G.; McKee, V.; Nelson, J.; Teat, S.J.; Clegg, W. *J. Chem. Soc. Dalton Trans.* **1998**, 1837–1843; Drew, M.G.B.; Harding, C.J.; McKee, V.; Morgan, G.G.; Nelson, J. *J. Chem. Soc. Chem. Commun.* **1995**, 1035–1038.
(42) Quinonero, D.; Garau, C.; Rotger, C.; Frontera, A.; Ballester, P.; Costa, A.; Deya, P.M. *Angew. Chem. Int. Ed.* **2002**, *41*, 3389–3392; Mascal, M.; Armstrong, A.; Bartberger, M.D. *J. Am. Chem. Soc.* **2002**, *124*, 6274–6276; Alkorta, I.; Rozas, I.; Elguero, J. *J. Am. Chem. Soc.* **2002**, *124*, 8593–8598; Brooker, S.; White, N.G.; Bauzá, A.; Deyà, P.M.; Frontera, A. *Inorg. Chem.* **2012**, *51*, 10334–10340.
(43) Housecroft, C.E.; Sharpe, A.G. *Inorganic Chemistry*, 2nd ed.; Pearson Education Limited: Essex, UK, 2005.
(44) Blessing, R.H. *Acta Crystallogr., Sect. A* **1995**, *51*, 33–38; Sheldrick, G.M. Göttingen, **1996**.
(45) Sheldrick, G.M. *Acta Crystallogr. A Found. Crystallogr.* **2008**, *A64*, 112–122.